Hearing Research 398 (2020) 108090

Contents lists available at ScienceDirect

Hearing Research

journal homepage: www.elsevier.com/locate/heares

Research Paper

Short and long-term adaptation in the auditory nerve stimulated with high-rate electrical pulse trains are better described by a power law

M.J. van Gendt[a,*], M. Siebrecht[a], J.J. Briaire[a], S.M. Bohte[b], J.H.M. Frijns[a]

[a] ENT-Department, Leiden University Medical Centre, PO Box 9600, Leiden 2300 RC, The Netherlands
[b] CWI, Center for Mathematics and Informatics, Amsterdam, The Netherlands

ARTICLE INFO

Article history:
Received 28 May 2020
Revised 2 September 2020
Accepted 22 September 2020
Available online 2 October 2020

Keywords:
Cochlear implants
Neural model
Adaptation
Sensorineural hearing loss

ABSTRACT

Despite the introduction of many new sound-coding strategies speech perception outcomes in cochlear implant listeners have leveled off. Computer models may help speed up the evaluation of new sound-coding strategies, but most existing models of auditory nerve responses to electrical stimulation include limited temporal detail, as the effects of longer stimulation, such as adaptation, are not well-studied. Measured neural responses to stimulation with both short (400 ms) and long (10 min) duration high-rate (5kpps) pulse trains were compared in terms of spike rate and vector strength (VS) with model outcomes obtained with different forms of adaptation. A previously published model combining biophysical and phenomenological approaches was adjusted with adaptation modeled as a single decaying exponent, multiple exponents and a power law. For long duration data, power law adaptation by far outperforms the single exponent model, especially when it is optimized per fiber. For short duration data, all tested models performed comparably well, with slightly better performance of the single exponent model for VS and of the power law model for the spike rates. The power law parameter sets obtained when fitted to the long duration data also yielded adequate predictions for short duration stimulation, and vice versa. The power law function can be approximated with multiple exponents, which is physiologically more viable. The number of required exponents depends on the duration of simulation; the 400 ms data was well-replicated by two exponents (23 and 212 ms), whereas the 10-minute data required at least seven exponents (ranging from 4 ms to 600 s). Adaptation of the auditory nerve to high-rate electrical stimulation can best be described by a power-law or a sum of exponents. This gives an adequate fit for both short and long duration stimuli, such as CI speech segments.

1. Introduction

Cochlear implants (CIs) are implantable hearing devices for people with severe to profound hearing loss. CIs generally allow good speech understanding, but outcomes are highly variable and speech perception remains challenging in more complex listening situations. Many different sound-coding strategies have been introduced in the last decade to improve sound coding, but performance on perception tests has not improved significantly (Zeng, 2017). New stimulation strategies are commonly investigated in psychophysical experiments and clinical trials, which is time-consuming for both the patient and researcher and does not provide insight into physiological characteristics underlying the large variability in perception scores. Alternatively, strategies could be evaluated using computational models. A variety of models are currently available that can simulate responses of the auditory nerve to electrical stimulation.

Models that simulate responses of the auditory nerve to electrical stimulation can be classified as phenomenological or biophysical. Biophysical models, which describe physiological elements of the neuron in detail, have been shown to reproduce deterministic threshold characteristics and refractory behavior in response to a stimulation of several milliseconds, with arbitrary pulse shapes (Dekker et al., 2014; Frijns et al., 2001; Frijns and ten Kate, 1994; Kalkman et al., 2015; O'Brien and Rubinstein, 2016). Methods to biophysically model more complex neural behavior, such as stochasticity and the effects of long temporal spiking history, have also been suggested. These methods provide insight into the physiological processes, but have the disadvantage of requiring many parameters to be fitted and consume great computational power (Negm and Bruce, 2014; O'Brien and Rubinstein, 2016; Woo et al.,

* Corresponding author.
E-mail address: m.j.van_gendt@lumc.nl (M.J. van Gendt).

https://doi.org/10.1016/j.heares.2020.108090

2010, 2009). Efficient computation of the neural responses of all ~30,000 auditory nerve fibers is fundamental to predicting perception outcomes. Alternative to biophysical models, phenomenological models, that describe the behavior of the neuron empirically, can be used efficiently for these purposes. Stochasticity is such a phenomenon that can be included (Bruce et al., 1999b, 1999a), and more recently adaptation has been included in phenomenological models (Boulet et al., 2016; van Gendt et al., 2019, 2016). The effect of adaptation increases with stimulus duration and rate (van Gendt et al., 2017, 2016). Therefore, in simulations of neural responses to segments of speech, which are of long durations, adaptation becomes relevant. Contemporary CIs use pulse rates of 800–2000 pps, but depending on the spatial spread single neurons may be stimulated by higher rates.

Single fiber auditory neuron recordings in response to long duration electrical stimulation, which can be used for verification, is available only for high pulse rates (5 kpps). For lower stimulus rates adaptation is expected to have a smaller effect. It has been suggested that high rate pulse trains can be used as desynchronizing pulse trains (Rubinstein et al., 1999). In the healthy auditory nerve there is spontaneous activity, which yields linear behavior also for low stimulus levels. Electrically stimulated auditory nerve fibers, however, respond highly synchronized, diminishing the dynamic range. To overcome this, it has been suggested to first stimulate the auditory nerve with a high-rate (e.g., 5kpps) pulse train, bringing all fibers in a refractory or adapted state, after which spiking will be less coherent.

Adaptation is a well-known phenomenon in general neuroscience that is particularly well-studied in the visual system. Adaptation has been shown to maximize information transmission (Barlow, 1961; Wark et al., 2007). Neural adaptation dynamics depend on the stimulus history (de Ruyter van Steveninck et al., 1986). Neurons not only adapt to stimulus gain, but to a range of stimulus statistics, so that stimuli in a dynamic environment are represented most efficiently (Brenner et al., 2000). Such statistics may be very different over different durations of stimulation. After long durations of stimulation, the dynamics of adaptation in neural systems in general are often better described by a power law than an exponent (Toib et al., 1998). In the fly's visual system, adaptation was demonstrated to occur at different time scales; short time scales are necessary for optimal information encoding of rapid stimulus variations within an ensemble, whereas long time scales adjust the rate and statistics of the firing pattern to provide information about the ensemble of the stimulus (Fairhall et al., 2001). A power law function can be approximated by a combination of a large number of exponential processes with a range of time constants (Drew and Abbott, 2006). Many natural processes decay and grow exponentially. Although neurons behave according to a power law, no individual biological processes that can be described by a power law have been detected in neurons (Drew and Abbott, 2006), and the dynamics probably arise physiologically from different exponential processes. Because of the power law dynamics, neurons are capable of adapting their responses to stimulus statistics over a wide range of time scales, from tens of milliseconds to minutes. Thus, adaptation has been shown to play a role in efficient coding of the continuously (rapidly or slowly), changing sensory world.

In the auditory system, adaptation is also a supposed mechanism for optimized information transmission (Clague et al., 1997; Epping, 1990). Neurons can adapt to stimulus statistics, such as sound level and variance (Dean et al., 2005; Wen et al., 2009). The dynamic range is adjusted to the range of presented sound levels, leading to high accuracy of the perception of differences in loudness, regardless of the large dynamic range spanned by the input levels. Auditory nerve responses to statistically varying acoustic input were well-replicated by a model that included power law adaptation (Zilany et al., 2009; Zilany and Bruce, 2006). This model showed that power law adaptation increases the dynamic range of the auditory neuron (Zilany and Carney, 2010). Auditory neurons also adapt in response to electrical stimulation (Heffer et al., 2010; Litvak et al., 2003; Zhang et al., 2007). This becomes especially apparent with stimulus durations >100 milliseconds, as is the case in pulse trains encoding speech segments. Thus, a model of the auditory nerve that simulates responses to electrical CI stimulation representative of speech should account for adaptation. Previously, a model combining the biophysical and phenomenological approaches was shown to accurately simulate spiking of the auditory nerve in response to electrical pulse trains of durations up to a few hundred milliseconds (van Gendt et al., 2019, 2017, 2016). In these studies, adaptation was modeled by increasing the threshold following each spike or pulse with a certain amplitude that exponentially decayed over time. Exponential spike adaptation and accommodation with a time constant of 100 ms was found to explain spiking behavior in response to both amplitude modulated and continuous amplitude pulse trains with duration up to 400 ms. This model, with a single exponent, successfully replicated responses, but its success was restricted to the limited stimulus ranges for which its parameters were optimized. The model has not been validated for longer duration stimulation. In addition, no studies have evaluated whether a power law, a single exponent, or a sum of exponents best describes the response of the auditory nerve to electrical stimulation.

As speech segments have durations of up to several seconds and a large dynamic range, it is important that the adaptation be correctly implemented in a model of neural responses to speech coding in CIs. The present study evaluated which model of adaptation best describes the responses of the auditory nerve to long duration stimulation. For this, recordings of the auditory neuron's responses to pulse trains with short and long durations were simulated with different models of adaptation. The used model builds on a previously developed computationally efficient model (van Gendt et al., 2017).

It is plausible to expect that more than one time-component is required to model long duration responses. This could be modeled as multiple exponentials, or, with less parameters, with a power law. This study investigates how both short- and long-term adaptation of auditory neurons to electrical stimulation can most adequately, physiologically realistic and computationally efficient be described and fitted.

2. Methods

Responses of the electrically stimulated auditory nerve were modeled using a combined biophysical and phenomenological model.

2.1. Deterministic thresholds

First, deterministic fiber thresholds (I_{det}) were calculated with a 3D volume conduction model and active nerve fiber model developed in the LUMC (Kalkman et al., 2015, 2014). The cochlear geometry is based on micro-CT data, the electrode array geometry is based on the HiFocus1J array (Advanced Bionics, Valencia, CA, USA) in lateral position. Deterministic thresholds were obtained for specific pulse shapes and pulse widths. In the current paper biphasic pulses with pulse-widths per phase of 18μs were used.

2.2. Phenomenological threshold adjustments

These deterministic thresholds were adjusted with stochasticity, adaptation, and accommodation using a phenomenological approach (van Gendt et al., 2017, 2016). For each nerve fiber,

Table 1
Parameters for optimization.

Parameter	Range
Accommodation amplitude (α_{acco}),%	0.004 – 0.014, step size: 0.002
Adaptation amplitude (α_{adap}),%	0.00 – 0.05, step size: 0.01
Offset, ms	1, 5, 20, 40
Exponent β	−1.2, −1.1, −1.0, −0.9

the stochastic threshold was taken from the normal distribution, $N(I_{det}, SD)$, with SD calculated with a relative spread (RS) as $SD = I_{det} \cdot RS$. Subsequently, refractoriness (R), as calculated with Eq. (1), was added to the stochastic threshold.

$$R = \frac{1}{1 - e^{\frac{-(t-\tau_{ARP})}{\tau_{RRP}}}}, \quad (1)$$

where τ_{ARP} and τ_{RRP} are the time constants for the absolute and relative refractory period, and t is the time since the last action potential. It was shown previously (van Gendt et al., 2017, 2016) that the adaptation behavior of the auditory nerve in response to electrical stimulation is a consequence of both sustained firing, referred to as spike adaptation (SA), and sustained stimulation, referred to as accommodation ($Acco$). Different models to described SA and $Acco$ are described below. The final threshold was calculated as follows;

$$I_{adj} = N(I_{det}, \sigma) \cdot R + SA + Acco \quad (2)$$

A spike was assumed to occur when: $I_{given} > I_{adj}$, where I_{given} is the stimulus current. The parameters for stochasticity, refractoriness, and single exponential adaptation were previously fitted (van Gendt et al., 2017, 2016). An overview of the parameters is given in Table 1 in the appendix. The present paper determined parameters for power law adaptation and multiple exponentials.

Single exponent adaptation

Adaptation was previously modeled with an exponential decay as in Eq. (3).

$$A = \alpha \cdot \sum_i SP \cdot e^{\frac{t-t_i}{\tau_a}} \quad (3)$$

α is the adaptation amplitude or the accommodation amplitude. SP, a spatial factor, is 1 for spike adaptation, and $0.03\% \cdot I \cdot \frac{I_{min}(electrode)}{I(electrode,\ fiber)}$ for accommodation, $I_{min}(electrode)$ is the threshold for the fiber most sensitive to the used electrode, and $I(electrode, fiber)$ is the threshold for a particular fiber to that electrode. For spike adaptation i refers to the last spike, for accommodation i refers to the last stimulus pulse given.

Power law adaptation

The power law function was implemented in the neural model as in Eq. (4):

$$PLA(t) = \alpha \cdot \sum_i SP \cdot (t - t_i + offset)^{\beta}, \quad (4)$$

where i, α and SP are the same as above, offset represents a shift in the power law function, and β is the power component for the power law. Offset and β were assumed equal in both spike adaptation and accommodation.

Power law approximation with multiple exponents

Power law adaptation can be approximated by multiple exponents (Drew and Abbott, 2006). This was implemented here as in Eq. (5) for one exponent and Eq. (6) for multiple (k) exponents:

$$ExpA(t)_k = \alpha \cdot \sum_i SP \cdot e^{\frac{t-t_i}{\tau_a}} \quad (5)$$

$$ExpA(t) = \sum_k ExpA(t)_k, \quad (6)$$

where i, α and SP are the same as above, and τ refers to the time constant for the exponential adaptation.

2.3. Model optimization

The parameters for the single exponent adaptation model were previously fitted (van Gendt et al., 2017, 2016), and the formulas and optimal parameters are given in Appendix A. The power law adaptation model was fitted to two different data sets. The first data set consisted of the responses of one fiber to short duration (400 ms) amplitude-modulated electrical pulse trains with five different stimulus amplitudes (Hu et al., 2010) (Fig. 2). For this short duration data, similar to the recordings, stimulation amplitudes were set to a certain relative amplitude compared to the threshold, which was defined as the stimulus amplitude that yielded a response of 100 spikes/s in the first bin. Similar to the recordings by Hu et al. (2010), the stimulus duration was 400 ms, bin-width 50 ms, pulse rate 5000 pps, modulation frequency 100 Hz, and modulation depth 10%. The second data set consisted of the responses of seven different fibers to long duration (600 s) continuous amplitude electrical pulse trains (Litvak et al., 2003). For this long duration data, the measurements of the seven different fibers (Fig. 1) were replicated. Stimulus levels that elicited the same simulated discharge rate in the initial bin as in the recordings were chosen. The duration was 600 s, the rate was 5000 pps, and bin-width was 1 second. Responses of fiber 1200 (located roughly 180° from the round window) to stimulation of the nearest electrode contact were simulated.

2.3.1. Parameter search

Simulations were performed for both data sets using a range of parameters (Table 1). Combinations of different parameter settings in the range (i.e., 432 unique parameter sets) were used to simulate both datasets. Refractoriness and relative spread were set to the average values as published by van Gendt et al. (2017). See Appendix A for an overview of these parameters.

2.3.2. Minimal normalized rms error

Values were visually extracted from the published data recordings for the measured discharge rates in all different bins. Differences between simulated and measured discharge rates were calculated using the normalized root mean square error (NRMSE), normalization was done by dividing by the range of the measured rates per stimulus amplitude. The NRMSE was calculated for each stimulus amplitude (a) as in Eq. (7).

$$NRMSE_a = \frac{\sqrt{\sum_{n=1}^{N} (\bar{r}_a - r_a)^2}}{r_{a,\ max} - r_{a,\ min}} \quad (7)$$

where for N bins, r is the measured rate and $\bar{r}$ the simulated rate.

The NRMSE values for all stimulus levels were averaged. For both data sets, the parameter set with minimal error was defined. These parameter sets were used to simulate responses to the other data set for which it was not optimized. An optimal parameter set for both conditions combined was defined as the set yielding the minimal average NRMSE of both data sets. In addition, in the long duration data, seven different fibers were used, and the optimal parameter set was defined for each individual fiber. A sensitivity analysis was performed in which the effect of parameter variations on the NRMSE was investigated.

2.4. Approximating the power law fit with multiple exponents

The optimal power law parameter set was matched to a sum of exponents using least squares optimization. The number of exponents (n) for this fit was increased until 5 or, if no good fit was found with 5 exponents, until the NRMSE did not decrease more

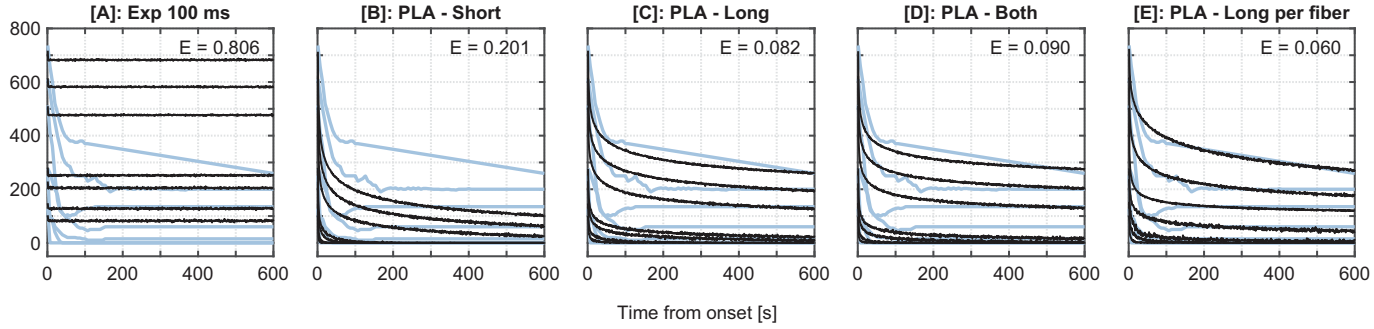

Fig. 1. Discharge rates in response to long duration stimulation (600 s). The simulations are plotted in black. The visually extracted data from Litvak et al. (2003) is plotted in blue in each graph. The E in the upper right corner refers to the mean NRMSE for all fibers. Simulated discharge rates are calculated with the 100 ms exponential model [A], with the power law model optimized for the short duration data [B], with the power law model optimized for the long duration data [C], with the power law model optimized for both the short and long duration data [D] and with the power law model optimized per fiber for the long duration data [E].

Table 2
Optimal parameter sets yielding the smallest NRMSE averaged for the different stimulus amplitudes on the short duration data (Short), the seven different fibers used in the long duration data (Long), for both errors averaged (Both) and per fiber (F) in the long duration data.

	Short	Long	Both	F1	F2	F3	F4	F5	F6	F7
Offset, ms	20	5	20	5	5	5	5	40	20	40
Exponent β	−1	−1	−1.1	−0.9	−0.9	−1.1	−1	−1.2	−1	−0.9
α accommodation [x 10^{-4}% of stimulus]	10	6	8	6	4	4	4	12	6	4
α adaptation [% of threshold]	0.03	0.02	0.02	0.02	0.01	0.00	0.01	0.05	0.02	0.01

than 10% with an extra exponent. In order to limit the search space for the least squares-optimization of the parameters for the set of exponents, the power law kernel was divided into n parts of equal log-length. The longest exponent was fitted first and only on the last part of the power law kernel. The second longest exponent was fitted on the last two parts of the power law kernel taking the contribution of the longest exponent into account. Following this pattern, the shortest exponent was fitted last on the entire duration of the power law kernel taking all other exponents into account. This method ensured that all exponents were properly normalized. The log spacing ensured that the exponents overlapped equally with each other.

3. Results

The optimal parameter set was defined as the combination of parameters that yielded the smallest NRMSE. Table 2 shows these parameter sets optimized for the short and long duration data and those combined (columns Short, Long and Both respectively), and for each of the individual fibers of the long duration data (F1 – F7).

3.1. Comparison of model simulations to recordings

3.1.1. Long duration simulations

For the long duration simulations, measured and simulated spike rates over the course of the stimulus are plotted in Fig. 1. Data were recorded from seven different fibers from one animal (Litvak et al., 2003). The two units with the lowest response amplitudes stopped discharging after 1–2 min, the other five units exhibited adaptation over the first 100 s followed by either slow adaptation or a steady response. For comparison, the simulations for the previously published model with an exponent of 100 ms is shown in Fig. 1A. The power law adaptation simulations with the optimal parameter set (Table 2) for the short and long duration data are shown in Fig. 1B and 1C respectively, 1D shows the simulations with the parameter set that yielded the minimal combined error. Fig. 1E shows the power law fit when the optimal parameter set is chosen per fiber.

The simulations with exponential adaptation only showed an initial, small decrease in spike rate, whereas all power law adaptation models demonstrated a continuous spike rate decrease over the course of the stimulation (Fig. 1). Quantitatively, the power law outperformed the model with exponential adaptation, as reflected in the NRMSE value of 0.806 for exponential adaptation, 0.201 for power law adaptation with the parameter set optimized for the short duration data, 0.082 optimized for the long duration data set, 0.090 for both data sets and 0.060 optimized per fiber. Both the parameter set optimized for this particular data and the parameter set optimized for the short duration data yielded a substantial improvement in predicting the discharge rate relative to single exponent. The best replication was obtained when optimized per fiber. The only difference between the recordings and these per-fiber-simulations was that the dip in the spike rate at approximately 50 to 150 s was not replicated by the model.

3.1.2. Short duration, amplitude-modulated simulations

To investigate which model best described the discharge rates and modulation following behavior in response to short duration amplitude-modulated pulse trains, the recordings from Hu et al. (2010) were simulated. The single exponent model and the power law models optimized for the short duration data and for the long duration data were used. For ease of comparison, recordings and simulations are plotted together in Fig. 2.

For the spike rates, the exponential adaptation yielded an NRMSE of 0.094. The power law model with the parameters optimized for this data and the combined data sets had NRMSE's of 0.065 and 0.068 respectively, outperforming exponential adaptation, whereas the parameters optimized for the long duration data only performed quantitatively worse, with an NRMSE of 0.134. For the VS, the single exponent model performed better than any of the power law models. Vector Strength measures periodicity in the neural response to a periodic input. The vector strength in the models is above zero but lower than the recordings. This means that some periodicity is maintained in the modeled responses, but not as much as in the recordings.

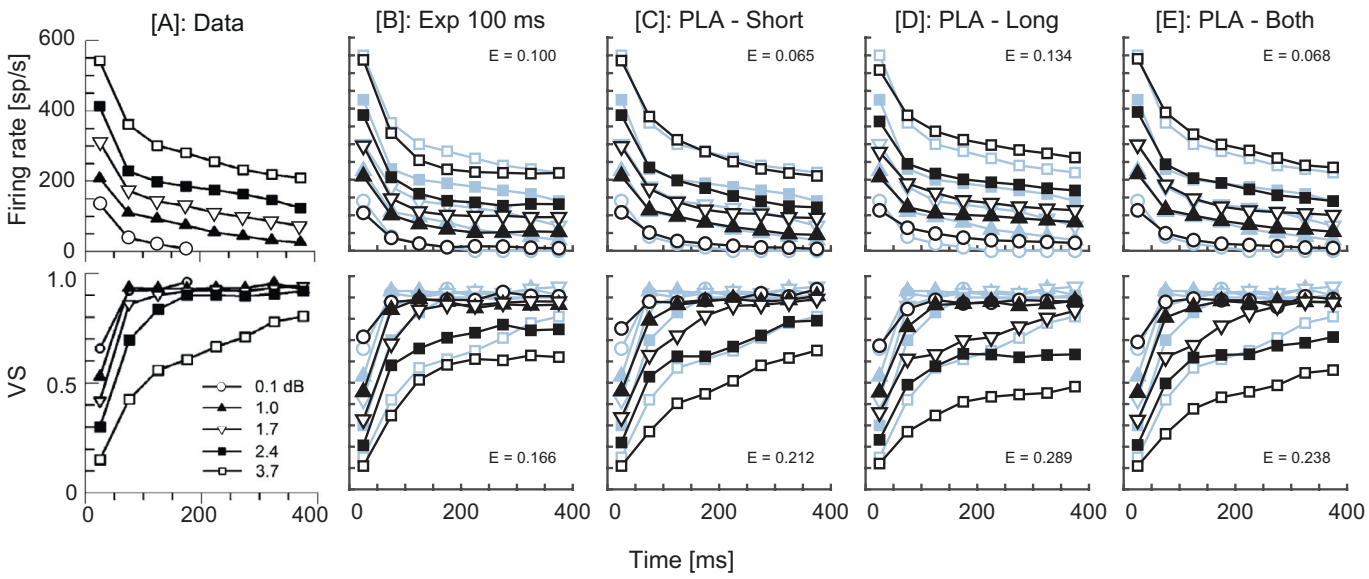

Fig. 2. Simulation of responses to short duration, amplitude-modulated pulse trains. Upper row shows spike rates determined in bins of 50 ms in response to five different stimulus amplitudes. The lower row shows vector strengths obtained from the same bins. For clarity, the recorded data are plotted separately in [A], and in [B-E] in gray-blue in the background (data from Hu et al., 2010, reprinted with permission). The numbers in the lower right corner in [A] indicate amplitudes relative to the threshold. In [B]-[E] simulations are plotted in black. Simulations were modeled with exponential adaptation, single exponent (100 ms) in [B], with the parameter set optimized for the short data in [C], with the parameter set optimized for the long duration data in [D], and with the parameter set optimized for both data sets in [E]. The optimal parameter sets are given in table 2.

3.2. Sensitivity analysis

To find the parameter sets yielding the minimal NRMSE, simulations were performed with a range of stimulus parameters. To investigate how the error was affected by the variation in the parameters, a sensitivity analysis was performed. The sensitivity to the adaptation and accommodation parameters was investigated by plotting them for each exponent and offset combination, and the sensitivity of the exponent and offset parameters was investigated by plotting them for each adaptation and accommodation combination. The resulting graphs including the optimal parameters are shown in Fig. 3.

The patterns in Fig. 3 are different for the short and long duration data. For long duration data, larger accommodation values led to strong errors, which was not seen in the short duration data. The short duration data exhibited a combined effect of adaptation and accommodation amplitudes; larger adaptation amplitudes required smaller accommodation amplitudes for similar errors. Furthermore, we identified an entangled effect of offset and β in the short duration simulations that was not seen in the long duration simulations. In the long duration data, the exponent influenced the error much more than the offset.

3.3. Fitting the power law with multiple exponents

3.3.1. Short duration fits with multiple exponents

The actual physiological processes underlying adaptation likely have exponential dynamics, but together behave in line with power law dynamics. Therefore, we investigated how many exponential processes would be required to explain the data. Each added exponent adds two new parameters to the parameter space that needs to be fitted. Fitting with several parameters can lead to overfitting or lack of convergence. Moreover, running simulations of the history-dependent neural responses with multiple exponents requires tremendous computational power. Alternatively, the exponential parameters can be fitted on the power law function that, in turn, was fitted on the data. Here, the minimum number of exponents needed to reliably simulate the recordings was tested. The time constants and weights for each number of exponents are given in Appendix B. The simulations of the short duration data with multiple exponents are shown in Fig. 4.

Going from the fit with 1 exponent (τ=77 ms) to two exponents (τ_1= 23 and τ_2=212 ms) induced the largest improvement. The NRMSE decreased from 0.100 to 0.066, and a continuous decrease in the spike rate was seen, similar to the animal data. The VS also improved with the addition of a second exponent; the NRMSE decreased from 0.25 to 0.219. When the number of exponents increased further, no additional substantial improvement in replication of the data was seen.

3.3.2. Long duration fits with multiple exponents

In a similar approach as with the short duration data, the long duration data were fitted with exponents. The simulations with 1, 5 and 7 exponentials are shown in Figs. 5A-C. The NRMSE values for up to 10 exponentials are shown in Fig. 5D.

As can be seen in Fig. 5D, with up to seven exponents the fit improved; NRMSE decreased from 0.257 with the one fitted exponent to 0.079 with seven exponential functions. With seven exponents the taus ranged from 4 ms to 600 s, with approximately one order size difference between each tau. The NRMSE of 0.079 as found with seven exponents is similar to the NRMSE found with the power law fitted on the long duration (0.082, Fig. 1C).

4. Discussion

Power law and exponential models of adaptation were evaluated for their performance in simulating the responses of the auditory nerve to electrical pulse trains of different durations. Firing rates were better simulated with power law adaptation optimized on both data sets combined than with exponential adaptation. For both data sets, when optimized for the data set itself the best results were obtained. The power law parameters optimized

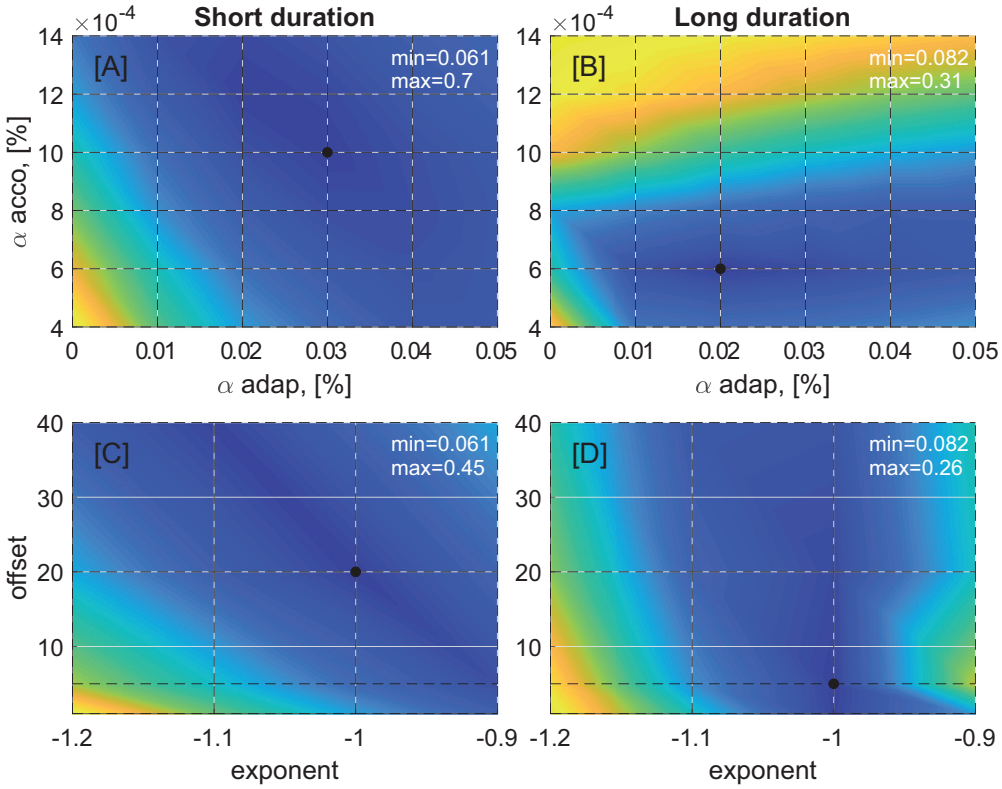

Fig. 3. NRMSEs for the short duration data (left) and long duration data (right). Color coding ranges from the minimal error in blue to the maximal error in yellow. The minimal and maximal values are included in each sub-figure. At all intersections of the dotted lines, responses were calculated, and between those points is interpolated. The following parameters were set so that the optimal value was included in each sub-figure: [A] offset = 20 ms, exponent = −1; [B] offset = 5 ms, exponent = −1; [C] adaptation = 0.03%, accommodation = 10 × 10–4%; and [D] adaptation = 0.02%, accommodation = 6 × 10–4%. (For interpretation of the references to colour in this figure legend, the reader is referred to the web version of this article.)

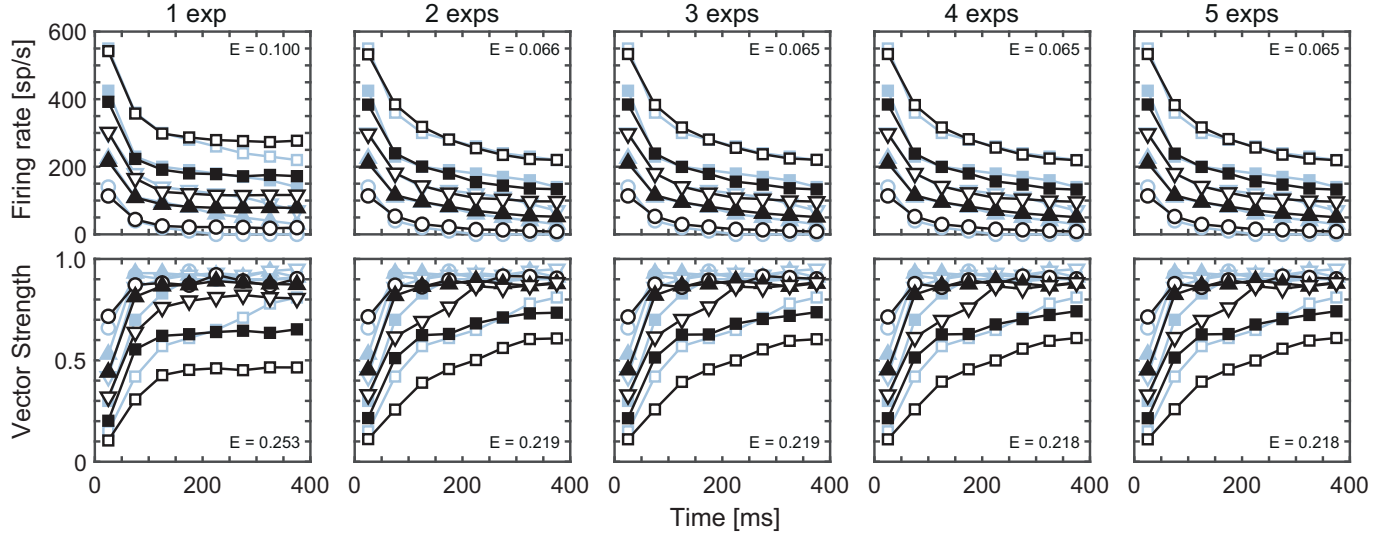

Fig. 4. Simulations with adaptation as sums of exponential functions, compared to the short duration data (Hu et al., 2010). Results of the simulations are shown in black, and the experimental counterparts as published by Hu et al. in gray-blue. The number of exponents to model the adaptation varied from 1 to 5. The exponential components were fitted to a power law function with the optimal parameters to fit the short duration data itself; beta = −1 and offset = 20 ms.

for short duration data also predicted the long duration data reasonably well, but short duration data simulated with the parameters for long duration data yielded a fit worse than the exponential. Vector strength was best simulated with exponential adaptation, but was in all simulations smaller than in the recordings. For individual fibers, slightly different parameter sets were found. The power law could be fitted with multiple exponents, which is physiologically more realistic. When enough exponents were included, this yielded similar responses as with the power law. The number of required exponents depended on the duration of stimulation. The effect of long duration stimulation is important because relevant temporal segments, such as sentences, are in the order of seconds rather than milliseconds, and regular CI usage will last a day. With improved models of adaptation as suggested here, extended

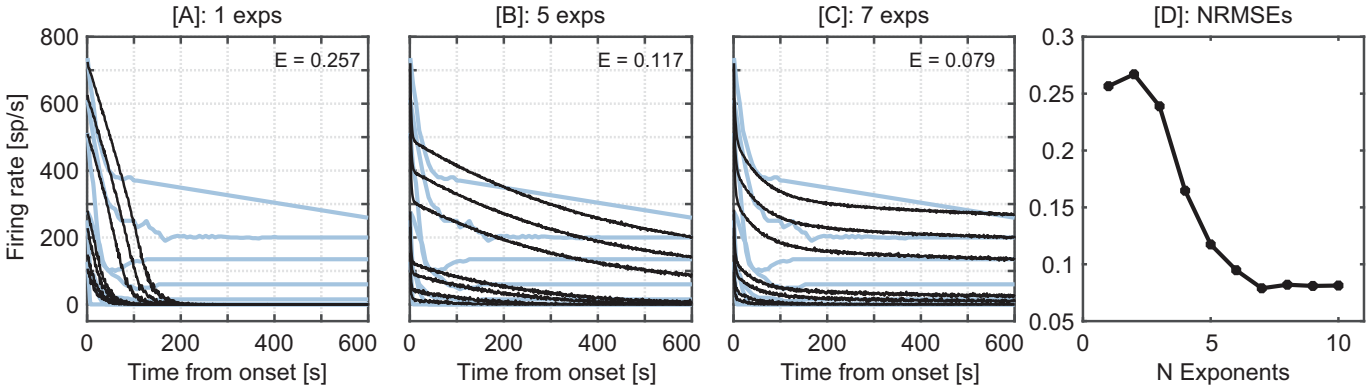

Fig. 5. Power law adaptation fitted with 1, 5 and 7 exponents in [A-C], the NRMSE compared to the long duration data (Litvak et al., 2003) for 1 up to 10 exponents is plotted in [D]. The results of the simulations are shown in black, and the experimental counterparts as published by Litvak et al. in gray-blue. Exponential functions were fitted to a power law function with $\beta = -1$ and offset = 5 ms.

with an interpretation model, the effect of sound-coding strategies for speech segments and longer duration stimulation can be evaluated. It will be particularly interesting to evaluate how the adaptation in the auditory nerve alters loudness perception and dynamic range. In the future, this improved understanding of neural adaptation could be used to test the performance of sound-coding strategies in long duration stimulation and provide suggestions on how to integrate adaptation in sound-coding strategies to optimally encode the acoustic environment.

4.1. Optimal power law parameters

Here, two different data sets were used to find the optimal parameter set, and an overall optimum parameter set was determined. The separate data sets were best described by a power law with an exponent of −1, the combined optimum was obtained with an exponent of −1.1. These values are in line with earlier studies of adaptation mechanisms in general computational neurosciences, and with specific studies on adaptation of the auditory nerve in response to acoustic stimulation (Zilany and Carney, 2010), where the exponent was found to be around −1. The parameter set found by minimizing the combined error outperforms the single exponential model for both the short and long duration data.

Power law adaptation has been argued to result in whitening of the neural responses, with the power law exponent optimizing information transmission by removing both short-range and long-range temporal correlations in spike trains (Pozzorini et al., 2013). For the individual fits, the exponents varied between −0.9 and −1.2 (Fig. 1D and Table 2). This spread in individual power law components suggests that the characteristic exponent depends on the frequency sensitivity of the neuron and the corresponding temporal correlations, thereby optimizing information transmission in the population of fibers. As seen in the sensitivity analysis for the short duration data (Fig. 3), there is a relationship between offset and exponent; with a smaller exponent, a smaller offset was required to yield minimal error. For the long duration data, such a relationship was not as clear. When the optimized power law was fitted to a single exponent, the resulting time constant (77 ms for the short duration data, and 60 s for the long duration data) was different from the time constant found in previous studies (100 ms) (van Gendt et al., 2017, 2016). A possible explanation for this is that, in previous studies, the exponent was found by directly optimizing on the data, whereas in the present study the exponent was found by fitting on the optimal power law. Moreover, previously, the time constant of 100 ms was based on a larger number of data sets. Previous studies combined the power law with exponential adaptation to ensure that adaptation on the shortest time scales was properly modeled (Zilany and Carney, 2010). In the model presented here, temporal neural behavior was described by both power law adaptation and refractory behavior, which is exponential with a time constant of approximately 1 ms. Parameters of the approximation with multiple exponents were obtained by a direct fit to the power law and minimizing the error. Alternatively, the error between expected output and simulated neural responses can be minimized directly, but requires much more computational effort. The computational effort depended mostly on stimulus duration and level, and was comparable for power law and exponential adaptation.

4.2. Biophysical origins of adaptation

The dynamics of adaptation in the auditory nerve in response to electrical stimulation, and more specifically the dynamics of power law adaptation, can be attributed to underlying phenomena with exponential dynamics. Generally, many biological processes cannot be described by a single exponential time constant, but rather by a sum of exponents with a wide range of time constants. Such a sum yields a single power law, which has been applied to model adaptation in neural systems (Anderson, 2001; Thorson and Biderman-Thorson, 1974). Up to this date it is unclear which biophysical processes cause power law adaptation and whether this is a single process or multiple processes operating on different time scales (Pozzorini, 2014). It has been suggested to be related to ion channel- (Teka et al., 2016; Toib et al., 1998), synaptic- (Fusi et al., 2005), and psychophysical dynamics (Fairhall et al., 2001; Zilany et al., 2009). The synaptic mechanism can be caused either by depletion of presynaptic neurotransmitters, or desensitization of post-synaptic receptors (Zilany et al., 2009). With electrical stimulation of the auditory nerve and recorded peripherally, as in this study, no synapse mechanisms or complex neural networks have been in place. Rather, the power law response in the recordings replicated here is an effect of adaptation in the behavior of the ion channels in the membranes of the auditory neurons.

Ion channels can show power-law dynamics under the assumption of a large number of hidden states (Ben-Avraham and Havlin, 1991; Teka et al., 2016), producing anomalous diffusion with power-law behavior. Such behavior has been shown to accurately capture single channel dynamics (Goychuk and Hänggi, 2004), with phenomenological power-law parameters relating to the transition probabilities between these hidden states. The exact parameters to be implemented in the kinetics of ion channels to yield the power law dynamics could be evaluated using a biophysical model.

Specific adaptation currents have been suggested in the literature, and have been related to different ion channels and time constants. The most well-known are the voltage-gated potassium (M-) currents, they may cause adaptation with time constants of a few milliseconds (Benda and Herz, 2003). Secondly, calcium-gated potassium currents have been shown to cause adaptation with time constants of around 50 milliseconds (Madison and Nicoll, 1984). A third, slower, mechanism is the slow recovery from inactivation of the sodium channels (Vilin and Ruben, 2001). The time constant of the slow inactivation process ranges from a few 100 ms up to tens of seconds (Benda and Herz, 2003; Blair and Bean, 2003). Moreover, a model study showed that hyperpolarization-activated cation and low-threshold potassium ion channels may play a role in adaptation with a time scale around 100 ms (Negm and Bruce, 2014). An after hyperpolarization, adaptation current may be generated by a cascade of exponential processes (Drew and Abbott, 2006). The number of relevant processes, the time scales involved, and the parameters required to couple the different processes depend on the duration of stimulation.

4.3. Implications of power law adaptation behavior

Power law adaptation provides an improved dynamic range and enhanced representation of stimulus dynamics (Fairhall et al., 2001; Mensi et al., 2016). The slow components of adaptation provide information about the context or stimulus statistics, whereas the fast components provide information about the rapid stimulus variations (Fairhall et al., 2001). Because of the slow variations, the human auditory system is sensitive to a wide range of stimulus levels, including levels of soft speech and loud shouting. With power law adaptation, auditory neurons that adapt to sound-level statistics (Zilany and Carney, 2010) are more sensitive to amplitude modulations in the presence of a steady background noise (Zilany et al., 2009) and to abrupt changes, such as those reflected in oddball paradigms (Antunes et al., 2010). When the neuron is adapted to a certain sound level, small variations are better detectable, i.e., just noticeable differences become smaller. A previous modeling study showed that weaker adaptation reduces the vector strength and vice versa, but vector strength is the results of a complex interplay of adaptation, stochasticity and refractoriness (van Gendt et al., 2017). Power law adaptation has been suggested to improve dynamic range, or precision coding in a dynamic environment. The question is whether long term adaptation components would come at the expense of short-term components, yielding the drop in vector strength. Models developed so far slightly underestimate vector strength of phase locking properties of the electrically stimulated auditory nerve (Goldwyn et al., 2010; van Gendt et al., 2017). It would be of great value to further investigate what neural behavior could underlie this strong phase locking. Future simulations with amplitude modulated pulse trains with means slowly varying over time could demonstrate how power law adaptation affects precision coding in a dynamically changing environment.

The modulation rate of the speech envelope is 2 to 50 Hz (Rosen, 1992), and peaks at 3–5 Hz. These slow modulations are important for speech perception. Frequency modulations, often referred to as fine-structure, occur on much shorter time scales. These faster modulations in speech (milliseconds or less) convey information about prosody, melody, intonation, timbre, and the quality of speech. One can expect that, because power law adaptation improves precision coding in a dynamic environment, it also improves the perception of both of these cues. This could be evaluated in a follow-up study including amplitude-modulated signals with different modulation rates and switching stimulus levels.

In CIs, loudness is generally coded by charge, i.e., the amplitude or width of the stimulus pulse, by which a larger number of fibers are stimulated. For normal hearing, loudness increases with a compressive function of sound pressure, whereas for electrical stimulation, loudness increases with an expansive function for increasing stimulation (Vellinga et al., 2017). Moreover, the dynamic range in CI listeners is much smaller than that of normal hearing listeners. Compression can be employed to compensate for the steep build-up in loudness. In addition, in contemporary CIs, matching the dynamic range of naturally occurring sounds to the perceptual dynamic range is improved through the automatic gain control (AGC). The AGC adjusts the loudness cue according to the history of stimulus levels averaged over a certain amount of time, thereby improving the comfortable audibility of a wide range of stimulus levels. These systems are generally slow- or fast-acting or dual. Fast-acting systems aim to evoke the loudness perception most true to nature, whereas slow-acting systems are designed to maintain the audibility of the amplitude differences for the modulation rates conveying speech information (Boyle et al., 2009). With an ideal AGC, neural activation would replicate the situation of natural hearing, and the optimal dynamic range would be achieved. To further optimize existing AGC designs in this direction, the difference in adaptation dynamics between the normal hearing situation and the electrically stimulated degenerated auditory nerve could be established and accounted for by sound processing. The present study shows that power law dynamics best describe the adaptation in the electrically stimulated auditory nerve. Ideally, the dynamics and strength of adaptation of the auditory nerve in an individual CI user would be determined. Subsequently, the adaptation mechanism in the sound-coding strategy could be adjusted so that the stimulation pattern effectively yields activation similar to the normal hearing situation.

In real-life, a CI listener will wear the CI continuously. Although there will be moments of relative quiescence, adaptation will occur continuously to a larger or smaller extent. Consequently, models of the auditory nerve in response to electrical stimulation will have to be tuned to this. Psychophysical experiments generally start in quiet. This may lead to inherent changes within the duration of the experiments. This should be considered while designing an experiment. When one wants to use a desynchronizing pulse train to activate the neurons from an adapted situation (Rubinstein et al., 1999), the duration of stimulation must be evaluated. As can be seen from the recordings (Litvak et al., 2003), most fibers fire at a constant rate after a stimulus duration of around 200 s. This suggests that here the maximum adaptation is reached.

The pulse trains simulated in the current study had pulse rates of 5 kpps. Stimulus rates used in contemporary cochlear implants vary from 800 to 2000 pps, with new developments in the lower frequency range. Because of cross-over stimulation between electrodes, neurons are likely to be affected by much higher rates than the stimulus rates on single electrodes, notwithstanding the fact that there will be a large variability of stimulus rates at the site of the neurons. It has been shown that the stimulus rate has an effect on the spike rate decreases over time for short duration responses (Heffer et al., 2010; Zhang et al., 2007). Previous modeling work showed that such differences over time can be replicated with a single model with the same parameters (van Gendt et al., 2016). For long duration electrical stimulation, unfortunately, such experimental data of neural responses to a variety of stimulus rates is not available. Such data would enable validation of, or optimization of the power law parameters (alpha, beta and offset) for low rate pulse trains. To investigate the theoretical effect of power law adaptation on clinically used, lower rate pulse trains, responses to long duration stimulation with 800 and 1800 pps were simulated, results are shown in Fig. 6.

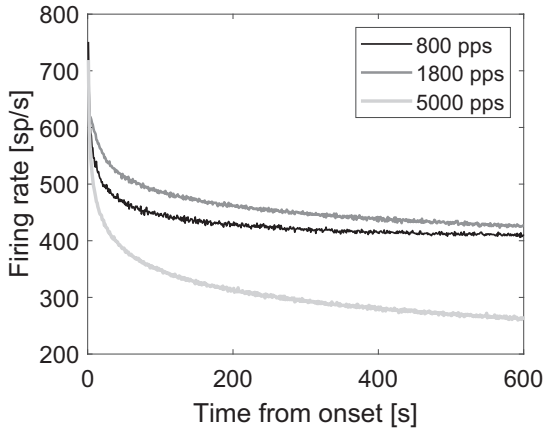

Fig. 6. Response rates simulated with power law adaptation (offset = 5 ms, exponent = −1, accommodation = 6 × 10–4% of stimulus, adaptation = 0.02% of threshold) for long duration pulse trains (600 s) with different stimulus rates; 800 pps (black), 1800 pps (middle gray) and 5000 pps (light gray). For all pulse trains the stimulus level was used that elicited the 720 spikes in the first second in response to the 5kpps pulse train.

Fig. 6 shows that also with lower rates the induced firing rates are expected to decrease over a long period of stimulation. The lower stimulation rates (800 and 1800 pps) had higher sustained firing rates than the response to 5000 pps, in which the neuron was supposedly less affected by adaptation and refractoriness. The sustained firing rates in response to 800 and 1800 pps are very similar. The exact response is the result of a complex interplay between refractory properties, accommodation, adaptation, and stimulus rate, and therefore dependent on stimulus rate in a nonlinear manner.

4.4. Limitations and suggestions for further research

The optimal parameter set was found via direct comparison of the simulated and recorded spike rates. However, especially for the long duration simulations, the model did not replicate some anomalous behavior of the recorded spike rates. Examples of this behavior were the dip in response rates around 50 ms and the continuous decrease in the strongest responding neuron. This latter observation may have been a result of continuing damage being done to the neuron due to the recording electrode, or displacement of the recording electrode. A larger number of these kinds of recordings from neural fibers would be required to determine whether this is an intrinsic neural behavior that should be modeled, or whether it is merely an effect of the recording method.

The short duration data fitted in this paper were all obtained from a single neuron. The other two fibers presented in Zhang et al. (2007) did not show the continuous decrease and were already reliably simulated by the model with a single exponent. Such inter-fiber differences indicate great variability between fibers in adaptation behavior. The improved fit on long duration data when optimized per fiber indicates that different fibers require a different parameter set and exhibit different neural behaviors. More experimental data are needed to obtain ranges for the parameters in auditory neurons. A previous study showed that the strength of adaptation may be related to the health of the auditory nerve (van Gendt et al., 2019). How the characteristics of the power law adaptation relate to neural health is unknown, but could be evaluated in a physiological study.

In a follow-up study, the effect of the amount of adaptation on long duration stimulation, especially speech segments, should be evaluated. An interpretation model that can relate the neural spiking to perceptual outcomes will be required. Hypotheses relating neural adaptation to increased dynamic range and loudness discrimination could be tested. In addition, the effect of diminished adaptation, in amplitude or temporal length, as may occur in a degenerated auditory nerve, on perceptual outcomes could be tested. Besides evaluating how the neural behavior can be expected to be related to perceptual outcomes, the model can also be used to compare different sound-coding strategies. After validation, new approaches to sound coding can be tested efficiently. With the model presented here, the performance of new designs and strategies in the perception of long duration speech segments can be evaluated.

Declaration of Competing Interest

None

Acknowledgements

This study was financially supported by the Heinsius-Houbolt Fund and Advanced Bionics Corporation.

Appendices

A. Exponential model formula and parameters

Table A.1

- Relative spread: $\sigma = I_{th} \cdot RS$
- Refractoriness: $R = 1 - e^{\frac{t-\tau_{ARP}}{\tau_{RRP}}}$
- Adaptation: $AF = \sum_i ampl_{adap} \cdot e^{\frac{t-t_i}{\tau_{adap}}}$
  - Every pulse: adaptation amplitude is increased:

Adaptation parameter:

$$ampl_{adap} = ampl_{adap}(oud) + \text{Adaptation amplitude} \cdot threshold\ (initial)$$

  - Every spike: adaptation amplitude is increased (accommodation):

Adaptation parameter (accommodation):

$$ampl_{adap} = ampl_{adap}\ (oud) + \text{Accommodation amplitude} \cdot stimulus\ current \cdot spatial\ factor$$

$$\text{Spatial factor} = \frac{I_{\min}(electrode)}{I(electrode,\ fiber)}$$

- Total model: $I_{final\_th} = N(I_{th}, \sigma) \cdot R + AF$

B. Power law approximation with exponents

Tables B.1, B.2

Table A.1
Model parameters.

Parameter	Value
RS	0.06
τ_{ARP}	0.4 ms
τ_{RRP}	0.8 ms
Within refractoriness stochasticity	5% of τ_{ARP}/τ_{RRP}
Adaptation amplitude	1% of threshold
Accommodation amplitude	0.03% of stimulus current · spatial factor

Table B.1
Fitted exponents and their weights to approximate the power law for short duration data.

1 exp in ms	77				
weight					
2 exps in ms	23	212			
weights	0.72	0.26			
3 exps in ms	17	80	376		
weights	0.61	0.28	0.13		
4 exps in ms	15	50	159	512	
weights	0.52	0.28	0.14	0.07	
5 exps in ms	14	36	93	237	606
weights	0.45	0.27	0.16	0.09	0.05

Exponential time constants and weights for the fit to power law with beta = −1 and offset = 20 ms.

Table B.2
Fitted exponents and their weights to approximate the power law for long duration data.

1 exp ms	6e5								
weights	2.5e-4								
2 exps ms	21	6e5							
weights	0.76	1.9e-4							
3 exps ms	10	150	6e5						
weights	0.86	0.13	1e-4						
4 exps ms	6.3	49	748	6e5					
weights	0.81	0.25	0.03	1.1e-4					
5 exps ms	5	26	197	2.8e4	6e5				
weights	0.71	0.35	0.067	7e-3	1e-4				
6 exps ms	3.8	17	88	628	7.8e3	6e5			
weights	0.61	0.41	0.11	0.021	2.3e-3	5.9e-5			
7 exps ms	4	14	68	407	3608	6.5e4	6e5		
weights	0.56	0.43	0.13	0.028	4.1e-3	2.9e-4	1.9e-5		
8 exps ms	3	12	48	239	519	134e2	897e2	6e5	
weights	.50	0.45	0.17	0.042	7.9e-3	1.0e-3	1.0e-4	2.8e-5	
9 Exps ms	2.8	9.4	35	140	710	4.1e3	2.2e4	1.1e5	6e5
weights	0.43	0.47	0.20	0.061	0.014	2.6e-3	4.5e-4	8.6e-5	2.3e-5
10 exps ms	2.4	7.3	23	82	320	1.4e3	7.1e3	3.1e4	1.4e5	6.0e5
weights	0.35	0.47	0.25	0.089	0.026	6.6e-3	1.3e-3	2.7e-4	6.2e-5	2.2e-5

Exponential time constants and weights for the fit to power law with beta = −1 and offset = 5 ms.

References

Antunes, F.M., Nelken, I., Covey, E., Malmierca, M.S., 2010. Stimulus-specific adaptation in the auditory thalamus of the anesthetized rat. PLoS ONE 5, 1–15. https://doi.org/10.1371/journal.pone.0014071.

Barlow, H.B., 1961. Possible Principles Underlying the Transformations of Sensory Messages. In: Sensory Communication, pp. 217–234.

Ben-Avraham, D., Havlin, S., 1991. Diffusion and Reactions in Fractals and Disordered Systems. Cambridge University Press. Springer Berlin Heidelberg https://doi.org/10.1007/978-3-642-51435-7.

Benda, J., Herz, A.V.M., 2003. A universal model for spike-frequency adaptation. Neural Comput. 15, 2523–2564. https://doi.org/10.1162/089976603322385063.

Blair, N.T., Bean, B.P., 2003. Role of tetrodotoxin-resistant Na+ current slow inactivation in adaptation of action potential firing in small-diameter dorsal root ganglion neurons. J. Neurosci. 23, 10338–10350. https://doi.org/10.1523/jneurosci.23-32-10338.2003.

Boulet, J., White, M.W., Bruce, I.C., 2016. Temporal Considerations for stimulating spiral ganglion neurons with cochlear implants. JARO - J. Assoc. Res. Otolaryngol. 17, 1–17. https://doi.org/10.1007/s10162-015-0545-5.

Boyle, P.J., Bchner, A., Stone, M.A., Lenarz, T., Moore, B.C.J., 2009. Comparison of dual-time-constant and fast-acting automatic gain control (AGC) systems in cochlear implants. Int. J. Audiol. 48, 211–221. https://doi.org/10.1080/14992020802581982.

Brenner, N., Bialek, W., De Ruyter Van Steveninck, R., 2000. Adaptive rescaling maximizes information transmission. Neuron 26, 695–702. https://doi.org/10.1016/S0896-6273(00)81205-2.

Bruce, I.C., Irlicht, L.S., White, M.W., O'Leary, S.J., Dynes, S., Javel, E., Clark, G.M., 1999a. A stochastic model of the electrically stimulated auditory nerve: pulse-train response. IEEE Trans. Biomed. Eng. 46, 630–637. https://doi.org/10.1109/10.764939.

Bruce, I.C., White, M.W., Irlicht, L.S., O'Leary, S.J., Dynes, S., Javel, E., Clark, G.M., 1999b. A stochastic model of the electrically stimulated auditory nerve: single-pulse response. IEEE Trans. Biomed. Eng. 46, 617–629. https://doi.org/10.1109/10.764938.

Clague, H., Theunissen, F., Miller, J.P., 1997. Effects of adaptation on neural coding by primary sensory interneurons in the cricket cercal system. J. Neurophysiol. 77, 207–220. https://doi.org/10.1152/jn.1997.77.1.207.

de Ruyter van Steveninck, R.R., Zaagman, W.H., Mastebroek, H.A.K., 1986. Adaptation of transient responses of a movement-sensitive neuron in the visual system of the blowfly Calliphora erythrocephala. Biol. Cybern. 54, 223–236. https://doi.org/10.1007/BF00318418.

Dean, I., Harper, N.S., McAlpine, D., 2005. Neural population coding of sound level adapts to stimulus statistics. Nat. Neurosci. 8, 1684–1689. https://doi.org/10.1038/nn1541.

Dekker, D.M.T., Briaire, J.J., Frijns, J.H.M., 2014. The impact of internodal segmentation in biophysical nerve fiber models. J. Comput. Neurosci. 37, 307–315. https://doi.org/10.1007/s10827-014-0503-y.

Drew, P.J., Abbott, L.F., 2006. Models and properties of power-law adaptation in neural systems. J. Neurophysiol. 96, 826–833. https://doi.org/10.1152/jn.00134.2006.

Epping, W.J.M., 1990. Influence of adaptation on neural sensitivity to temporal characteristics of sound in the dorsal medullary nucleus and torus semicircularis of the grassfrog. Hear. Res. 45, 1–13. https://doi.org/10.1016/0378-5955(90)90178-R.

Fairhall, A.L., Lewen, G.D., Bialek, W., de Ruyter van Steveninck, R.R., 2001. Efficiency and ambiguity in an adaptive neural code. Nature 412, 787–792. https://doi.org/10.1038/35090500.

Frijns, J.H.M., Briaire, J.J., Grote, J.J., 2001. The importance of human cochlear

anatomy for the results of modiolus-hugging multichannel cochlear implants. Otol. Neurotol. 22, 340–349.
Frijns, J.H.M., ten Kate, J.H., 1994. A model of myelinated nerve fibres for electrical prosthesis design. Med. Biol. Eng. Comput. 32, 391–398. https://doi.org/10.1007/BF02524690.
Fusi, S., Drew, P.J., Abbott, L.F., 2005. Cascade models of synaptically stored memories. Neuron 45, 599–611. https://doi.org/10.1016/j.neuron.2005.02.001.
Goychuk, I., Hänggi, P., 2004. Fractional diffusion modeling of ion channel gating. Phys. Rev. E - Stat. Phys. Plasmas, Fluids, Relat. Interdiscip. Top. 70, 9. https://doi.org/10.1103/PhysRevE.70.051915.
Heffer, L.F., Sly, D.J., Fallon, J.B., White, M.W., Shepherd, R.K., O'Leary, S.J., 2010. Examining the auditory nerve fiber response to high rate cochlear implant stimulation: chronic sensorineural hearing loss and facilitation. J. Neurophysiol. 104, 3124–3135. https://doi.org/10.1152/jn.00500.2010.
Hu, N., Miller, C.A., Abbas, P.J., Robinson, B.K., Woo, J., 2010. Changes in auditory nerve responses across the duration of sinusoidally amplitude-modulated electric pulse-train stimuli. J. Assoc. Res. Otolaryngol. 11, 641–656. https://doi.org/10.1007/s10162-010-0225-4.
Kalkman, R.K., Briaire, J.J., Dekker, D.M.T., Frijns, J.H.M., 2014. Place pitch versus electrode location in a realistic computational model of the implanted human cochlea. Hear. Res. 315, 10–24. https://doi.org/10.1016/j.heares.2014.06.003.
Kalkman, R.K., Briaire, J.J., Frijns, J.H.M., 2015. Current focussing in cochlear implants: an analysis of neural recruitment in a computational model. Hear. Res. 322, 89–98. https://doi.org/10.1016/j.heares.2014.12.004.
Litvak, L.M., Smith, Z.M., Delgutte, B., Eddington, D.K., 2003. Desynchronization of electrically evoked auditory-nerve activity by high-frequency pulse trains of long duration. J. Acoust. Soc. Am. 114, 2066–2078. https://doi.org/10.1121/1.1612492.
Madison, D.V., Nicoll, R.A., 1984. Control of the repetitive discharge of rat CA1 pyramidal neurones in vitro. J. Physiol. 354, 319–331.
Mensi, S., Hagens, O., Gerstner, W., Pozzorini, C., 2016. Enhanced sensitivity to rapid input fluctuations by nonlinear threshold dynamics in neocortical pyramidal neurons. PLoS Comput. Biol. 12, 1–38. https://doi.org/10.1371/journal.pcbi.1004761.
Negm, M.H., Bruce, I.C., 2014. The effects of HCN and KLT ion channels on adaptation and refractoriness in a stochastic auditory nerve model. IEEE Trans. Biomed. Eng. 9294, 1–12. https://doi.org/10.1109/TBME.2014.2327055.
O'Brien, G.E., Rubinstein, J.T., 2016. The development of biophysical models of the electrically stimulated auditory nerve: single-node and cable models. Netw. Comput. Neural Syst. 6536, 1–22. https://doi.org/10.3109/0954898X.2016.1162338.
Pozzorini, C., Naud, R., Mensi, S., Gerstner, W., 2013. Temporal whitening by power-law adaptation in neocortical neurons. Nat. Neurosci. 16, 942–948. https://doi.org/10.1038/nn.3431.
Pozzorini, C.A., 2014. Computational principles of single neuron adaptation PAR 6461.
Rosen, S., 1992. Temporal information in speech: acoustic, auditory and linguistic aspects. Philos. Trans. R. Soc. Lond. B. Biol. Sci. 336, 367–373. https://doi.org/10.1098/rstb.1992.0070.
Rubinstein, J.T., Wilson, B.S., Finley, C.C., Abbas, P.J., 1999. Pseudospontaneous activity: stochastic independence of auditory nerve fibers with electrical stimulation. Hear. Res. 127, 108–118. https://doi.org/10.1016/S0378-5955(98)00185-3.
Teka, W., Stockton, D., Santamaria, F., 2016. Power-law dynamics of membrane conductances increase spiking diversity in a Hodgkin-Huxley model. PLoS Comput. Biol. 12, 1–23. https://doi.org/10.1371/journal.pcbi.1004776.
Toib, A., Lyakhov, V., Marom, S., 1998. Interaction between duration of activity and time course of recovery from slow inactivation in mammalian brain Na+ channels. J. Neurosci. 18, 1893–1903. https://doi.org/10.1523/jneurosci.5392-08.2009.
van Gendt, M.J., Briaire, J.J., Frijns, J.H.M., 2019. Effect of neural adaptation and degeneration on pulse-train ECAPs: a model study. Hear. Res. 377, 167–178. https://doi.org/10.1016/j.heares.2019.03.013.
van Gendt, M.J., Briaire, J.J., Kalkman, R.K., Frijns, J.H.M., 2017. Modeled auditory nerve responses to amplitude modulated cochlear implant stimulation. Hear. Res. 351, 19–33. https://doi.org/10.1016/j.heares.2017.05.007.
van Gendt, M.J., Briaire, J.J., Kalkman, R.K., Frijns, J.H.M., 2016. A fast, stochastic, and adaptive model of auditory nerve responses to cochlear implant stimulation. Hear. Res. 341, 130–143. https://doi.org/10.1016/j.heares.2016.08.011.
Vellinga, D., Briaire, J.J., Van Meenen, D.M.P., Frijns, J.H.M., 2017. Comparison of multipole stimulus configurations with respect to loudness and spread of excitation. Ear Hear. 38, 487–496. https://doi.org/10.1097/AUD.0000000000000416.
Vilin, Y.Y., Ruben, P.C., 2001. Slow inactivation in voltage-gated sodium channels: molecular substrates and contributions to channelopathies. Cell Biochem. Biophys. 35, 171–190. https://doi.org/10.1385/CBB:35:2:171.
Wark, B., Lundstrom, B.N., Fairhall, A., 2007. Sensory adaptation. Curr. Opin. Neurobiol. 17, 423–429. https://doi.org/10.1016/j.conb.2007.07.001.
Wen, B., Wang, G.I., Dean, I., Delgutte, B., 2009. Dynamic range adaptation to sound level statistics in the auditory nerve. J Neurosci 29, 13797–13808 https://doi.org/29/44/13797 [pii]\r10.1523/JNEUROSCI.5610-08.2009.
Woo, J., Miller, C.A., Abbas, P.J., 2010. The dependence of auditory nerve rate adaptation on electric stimulus parameters, electrode position, and fiber diameter: a computer model study. J. Assoc. Res. Otolaryngol. 11, 283–296. https://doi.org/10.1007/s10162-009-0199-2.
Woo, J., Miller, C.A., Abbas, P.J., 2009. Biophysical model of an auditory nerve fiber with a novel adaptation component. IEEE Trans. Biomed. Eng. 56, 2177–2180. https://doi.org/10.1109/TBME.2009.2023978.
Zeng, F.-.G., 2017. Challenges in improving cochlear implant performance and accessibility. IEEE Trans. Biomed. Eng. 64, 1662–1664. https://doi.org/10.1109/TBME.2017.2718939.
Zhang, F., Miller, C.A., Robinson, B.K., Abbas, P.J., Hu, N., 2007. Changes across time in spike rate and spike amplitude of auditory nerve fibers stimulated by electric pulse trains. JARO - J. Assoc. Res. Otolaryngol. 8, 356–372. https://doi.org/10.1007/s10162-007-0086-7.
Zilany, M.S.A., Bruce, I.C., 2006. Modeling auditory-nerve responses for high sound pressure levels in the normal and impaired auditory periphery. J. Acoust. Soc. Am. 120, 1446. https://doi.org/10.1121/1.2225512.
Zilany, M.S.A., Bruce, I.C., Nelson, P.C., Carney, L.H., 2009. A phenomenological model of the synapse between the inner hair cell and auditory nerve: long-term adaptation with power-law dynamics. J. Acoust. Soc. Am. 126, 2390–2412. https://doi.org/10.1121/1.3238250.
Zilany, M.S.A., Carney, L.H., 2010. Power-law dynamics in an auditory-nerve model can account for neural adaptation to sound-level statistics. J. Neurosci. 30, 10380–10390. https://doi.org/10.1523/JNEUROSCI.0647-10.2010.